

Control Issues for Velocity Sourced Series Elastic Actuators

Gordon Wyeth

School of Information Technology and Electrical Engineering

University of Queensland

wyeth@itee.uq.edu.au

Abstract

The Series Elastic Actuator has been proposed as a method for providing safe force or torque based actuation for robots that interact with humans. In this paper we look at some outstanding issues in the implementation and control of Series Elastic Actuators. The study addresses issues in making the Series Elastic Actuator respond effectively in the presence of physical difficulties such as stiction, using a computation efficient controller. The improvement over previous implementations is achieved by treating the motor as a velocity source to the elastic element, rather than as a torque source.

1 Introduction

Actuation for robotics is a demanding task, requiring high torque and low speed, large peak power output for short periods, accurate feedback sensing, and suitability in shape, size and mass. With the advent of human robot interaction a new overriding concern arises: the inherent safety of the actuation mechanism and its compatibility with unpredictable and unstructured environments. Most robots use high impedance (stiff) position controlled actuators typical of industrial robot arms. Tasks such as walking are difficult when each footfall is seen as a collision with the ground by the rigid limb, especially on uneven or unknown surfaces. In unknown, unstructured human environments, low impedance (compliant) force controlled actuation improves safety [Zinn *et al*, 2004] and system controllability [Robinson *et al*, 1999].

Low impedance actuation means that the actuators source force (or torque) to the load, rather than commanding the load's position (or angle). Torque control of a geared motor can reduce the impedance of actuation at low frequencies, but cannot completely remove the high moment of inertia of the motor seen through the gearbox. Direct drive technologies (where the motor drives the load without a gearbox) can reduce but not eliminate this problem, and lead to much heavier and voluminous solutions. At higher frequencies above the control bandwidth, the mechanical impedance of either actuator is still very high. The magnitudes of impact loads, which are determined by high frequency impedances of the contact surfaces, are not attenuated [Zinn *et al*, 2004].

A Series Elastic Actuator (SEA) [Robinson, 2000] deliberately introduces compliance via a spring between the motor-gearbox and the load, and so has intrinsic low impedance. The spring's compression (measured simply with a distance sensor) is proportional to the spring torque. Using this measure for feedback creates a torque controlled actuator with inherently low output impedance. This concept is illustrated in Figure 1. A trade-off exists with the elastic element – increasing stiffness gives better high frequency control, but degrades the inherent safety and collision response properties. Related approaches such as Distributed Macro Micro (DM2) [Zinn *et al*, 2004] can overcome this trade-off at the cost of doubling the actuation and sensing requirements.

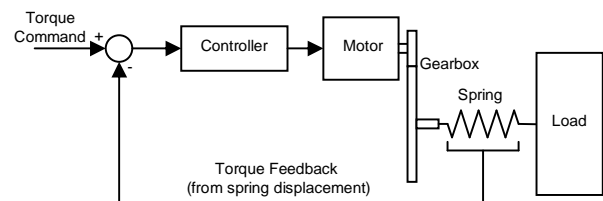


Figure 1: Series Elastic Actuator topology.

There have been some excellent examples of bird-like biped robots based on SEA [Paluska, 2000], but projects involving more complex use of the SEA have not been successful. Recently, insight into the reasons for this is given in reported shortcomings of current designs of SEA by the developers [Pratt *et al*, 2004]: (a) backlash between elements on the actuator creates instabilities, (b) gear stiction causes an initial slow response from the force loop, followed by an overshoot, and (c) the computational load is high leading to inadequate sampling rates.

Our aim is to develop a new variant of SEA that minimises the effect of the backlash between elements, overcomes the problems of stiction and is given adequate computational resources to perform the necessary control loops at high bandwidth. This paper shows the design and simulation of the new variant of the SEA which overcomes some of the existing problems with SEA implementation. The paper will show that the use of velocity control, rather than torque control, in the inner loop improves the design in a number of respects. The improvements are illustrated with a case study.

2 Previous SEA Studies

The control and implementation of Series Elastic Actuators have been approached from a number of perspectives. In [Pratt and Williamson, 1995] the concept is first introduced in the form of an electric motor in series with a spring for application in the Cog humanoid robot project [Brooks *et al*, 1998]. The spring in this model was a beam with a cross-shaped cross section. Deflection in the beam was measured using strain gauges. The motor was controlled using current control as the input to the motor, making the motor an effective torque source. The compensation scheme used both feedback from the strain gauges, and feedforward from the desired torque input to calculate a desired current for the motor. While the implementation demonstrated many of the desirable characteristics of a Series Elastic Actuator, there were a number of undesirable characteristics in the design. Backlash in the gearbox introduced some undesirable and unpredictable resonances in the closed loop response, and friction effects limited the effectiveness in providing large force bandwidth. In [Williamson, 1995], the authors note potential for improvement in the electronic design of the system.

The SEA was revisited in detail in [Robinson, 2000] again with the supposition that the motor is to be controlled as a torque source. The effects of friction and backlash are better quantified, and some guidelines for spring selection are introduced. The design presented in this paper were to be used in the M2 biped walker, although this robot never appeared to reach fruition. The actuators themselves formed the basis of the actuators for sale through Yobotics. Later work [Pratt *et al*, 2004] however describes similar problems to those seen by Williamson as outlined in Section 1.

3 Velocity Sourced SEA Design

In this paper, we change the paradigm for SEA design by treating the motor as a velocity source rather than as a torque source. This idea is suggested in [Robinson, 2000]. The reason that this idea becomes attractive is that a tight velocity control loop on the motor can overcome some of the undesirable effects of the motor and the gearbox. Velocity control is also more straightforward from an implementation perspective, unlike current control which is generally considered challenging.

3.1 Controlling a Velocity Sourced SEA

The principle of a velocity controlled SEA is shown in Figure 2. The motor has velocity feedback from an encoder that forms a tight loop for controlling the motor and gearbox. The velocity controller is tuned with no load attached, based on the assumption that the spring decouples any high-frequency torque disturbances on the SEA output, and that a well tuned velocity controller should be able to deal with low-frequency torque disturbances. With this tight velocity control loop in place, the motor can be treated as an effective velocity source, simplifying the ensuing torque control design. The procedure for designing the velocity control loop is well known and does not bear further exposition here. However, it is important to note that even in the presence of significant Coulomb and viscous friction losses in the motor and gearbox, a high performance velocity source can still be achieved in this fashion.

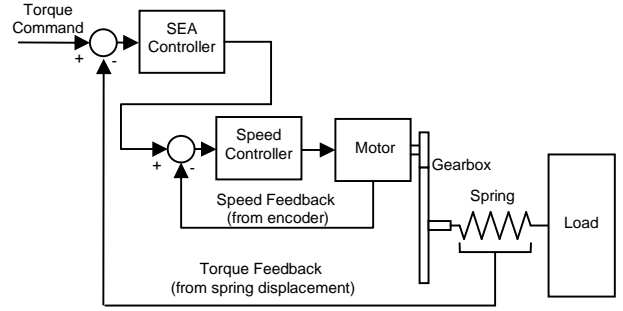


Figure 2: The inner velocity loop in the velocity source SEA helps to overcome problems with non-linearities and stiction.

3.2 Dynamics of a Velocity Sourced SEA

With the motor acting as a velocity source, the equations of motion associated with the SEA can be written. The spring deflection θ_s is a function of the motor speed ω_m and the position of the load θ_L :

$$\theta_s = \omega_m s - \theta_L$$

Assuming that the load has inertial properties, J_L , and is being controlled only by the actuator, that is, that there are no other torque sources affecting the load, then the position of the load is determined from the output torque applied to the load T_L :

$$\theta_L = T_L \frac{1}{J_L s^2}$$

But the torque applied to the load T_L is due solely to the deflection of the spring θ_s by:

$$T_L = K_s \theta_s$$

By combining these three expressions we can find the open loop transfer function from motor velocity to SEA output torque is given by:

$$\frac{T_L}{\omega_m} = \frac{K_s s}{s^2 + \frac{K_s}{J_L}}$$

where T_L is the output torque applied to the load, ω_m is the speed of the motor, J_L is the inertia of the load and K_s is the spring constant.

3.3 Choosing a Control Strategy

In closing the loop on this transfer function, we must consider the application. For a robotic application, the actuator must settle to the requested torque output quickly and accurately. The need to eliminate steady state error requires the introduction of two poles at the origin, and points to second-order PI compensation, using two cascaded PI compensators in the feedback path. For simplicity in this discussion, we choose to place the PI compensator zeroes at the same location. Later in the paper we will explore other options for zero placement.

The effect of closing the loop on a velocity sourced SEA with two cascaded PI compensators can be observed by looking at Figure 3. Figure 3 shows the root locus plots of a nominal system with a spring constant of 1 Nm/rad, for J_L set to first 0.1 kg.m² then 1 kg.m². It would seem from this plot that we might expect fast and accurate response by choosing values of K that bring two

of the poles close to the compensator zeroes, leaving the response dominated by the remaining pole. The position of the PI zeroes seems unimportant in such a design. This would be case, except that the motor with encoder feedback is not a pure velocity source; the motor velocity loop has its own pole. This pole has a potential adverse effect on the root locus as shown in Figure 4, where a pole at -10 rad/s has been introduced as an example.

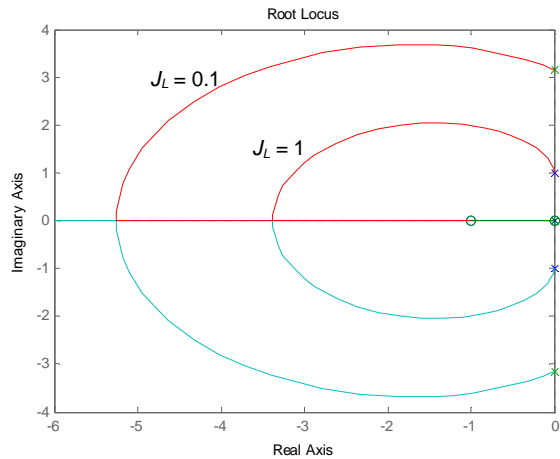


Figure 3: The root locus with an ideal velocity source for $J_L = 0.1 \text{ kg.m}^2$ and $J_L = 1 \text{ kg.m}^2$.

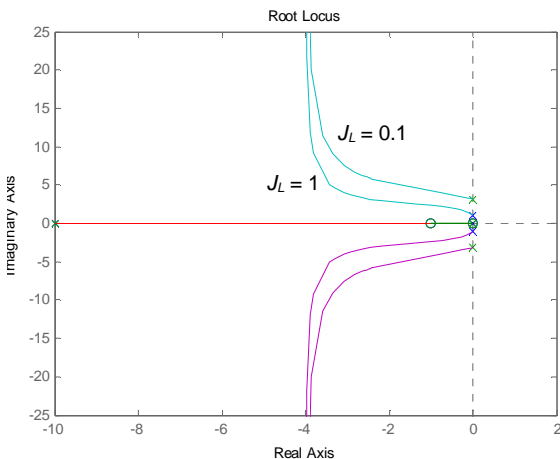


Figure 4: The impact on the root locus when a pole is placed in the velocity source.

Clearly, from this plot, it can be seen that the relationship between the open loop resonance of the load, the motor loop pole and the compensator zeroes is of critical importance if the system is to settle to a desired value quickly. There are also a number of non-linear issues that may affect overall system performance:

- noise in sensor feedback (particularly quantisation effects),
- sampling rate issues, and
- saturation of voltage and current to the motor.

All of these issues will be further investigated based on the case study below. After a linear systems analysis, results from non-linear simulation will illustrate that the velocity sourced series elastic actuator can overcome some of the problems that afflict torque sourced designs.

4 Case Study

We have designed a velocity sourced SEA intended for use in human-robot interaction applications. The design treats the series elastic element as a modular component that might be used with a range of motor systems, as are other transmission elements such as gearboxes. The design is pictured in Figure 5.

The series elastic element is 120 mm in diameter, and 98.5 mm in length, comprising a body 36 mm long, with 25 mm of output shaft and 37.5 mm of input shaft. The springs are valve springs usually used in motorbike engines. Each spring (coloured red in Figure 5) has a natural length 35 mm and an outer diameter of 25 mm, comprising 6 turns of 2.8 mm steel wire. The spring constants (verified using an Instron 4505 compression testing machine) are 19 N/mm. The four springs are arranged in the element provide a rotational spring constant of 138 Nm / rad. The springs are always in compression and remain linear in their behaviour.

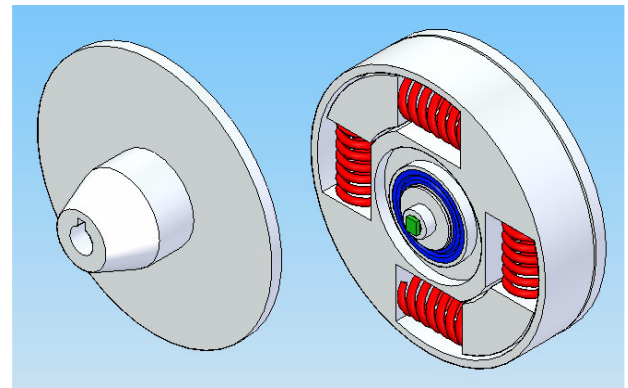


Figure 5: Series Elastic Element used in case study.

The deflection sensor is a critical element in the design, as noise or quantisation in the angle measurement impacts system performance dramatically. We have employed a Philips KMZ-41 Magnetic Field Sensor in a 150 kA/m field. The magnetic field is generated by 2 N38 grade $25 \times 12.5 \times 6 \text{ mm}$ block magnets magnetized through their 6mm thickness separated by an air gap of 16mm. This ensures magnetic field density greater than the required 100 kA/m and effectively saturates the sensor. Under these conditions the sensor can measure 180 degrees with 13 bit resolution, giving quantisation noise of 0.01 degrees. Given that the magnetic field is unlikely to be entirely homogeneous, and the sensor imperfectly centred in the field the angle measurement may have error as high as 0.1 degrees. This error affects the overall accuracy of the SEA as a torque source, but will not impact the dynamics. The sensor is the small green element in the centre of bearing in Figure 5.

This series elastic element could conceivably be combined with any number of velocity sources to form an SEA. In the following experiments the series elastic element is sourced from a Maxon RE35 90W 42V motor as used in the GuRoo humanoid robot project in our lab. The motor has an integrated GP42C 156:1 Planetary Gearhead and a HED-5540 500CPT encoder. The motor / gearhead / encoder has the relevant characteristics listed in Table 1 below.

Table 1: Table of properties of motor used to drive series elastic element.

Nominal Voltage	42 V
Terminal Resistance	2.07 Ω
Terminal Inductance	0.62 mH
Torque Constant	0.0525 Nm/A
Back EMF Constant	0.0525 Vs/rad
Rotor Inertia	6.96 x 10 ⁻⁶ kg.m ²
Reflected Gear Head Inertia	0.91 x 10 ⁻⁶ kg.m ²

Similarly, the series elastic element could be used to drive any number of loads. In this case, we will consider purely inertial loads in the range of 0.1 to 10 kg.m². This corresponds to typical loads that the robot might reasonably encounter if used in human robot interaction applications

5 Linear Design

The control system for the velocity sourced SEA was first investigated as a linear system in continuous time, which allowed rapid evaluation of a number of design ideas. This section outlines the results of that design process, which will form the basis for the discrete implementation in the following section.

5.1 Motor Velocity Controller

The motor velocity controller was tuned for rapid transient response and zero steady state error for a step input. The open loop transfer function (including the electrical pole formed by the motor inductance) is:

$$\frac{\omega_m(s)}{V(s)} = \frac{1.14 \times 10^7}{s^2 + 3339s + 59700}$$

A PI compensator is used to remove steady state error, with a zero at -200. Gain is then chosen to give good response, and to cancel the compensator's zero. With a gain of 0.27, the closed loop transfer function is:

$$\frac{\omega_m(s)}{\omega_d(s)} = \frac{3.192 \times 10^6 (s + 200)}{(s + 202)(s^2 + 3204s + 3.168 \times 10^6)}$$

With close cancellation of the compensator zero, the response is dominated by the complex poles with frequency 1.78 kHz and a damping ratio of 0.88. The step response is shown in Figure 6.

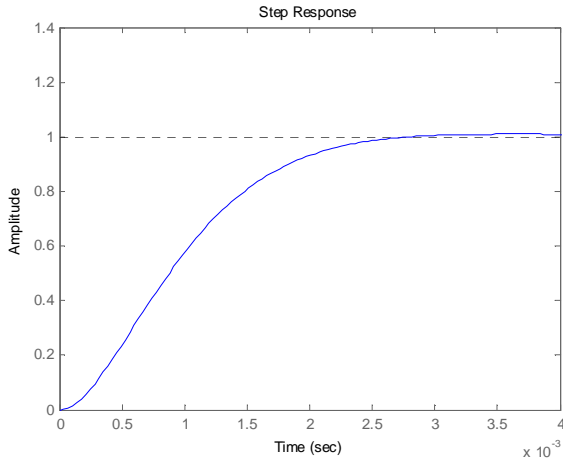


Figure 6: Step velocity response of inner motor loop.

5.2 SEA Controller

The transfer function for the velocity sourced SEA is readily derived for the reference case, noting that we also include the gear ratio, as the encoder feedback is measured from the un-g geared motor output:

$$\frac{T_L}{\omega_m} = \frac{1780^2 \cdot 138 / 156s}{(s^2 + 3130s + 1780^2)(s^2 + 1380)}$$

and for large loads:

$$\frac{T_L}{\omega_m} = \frac{1780^2 \cdot 138 / 156s}{(s^2 + 3130s + 1780^2)(s^2 + 13.8)}$$

Using the compensation principle described in Section 3.1, several experiments were performed searching for a good placement for the PI compensator zeroes, settling on zeroes at $-20 \pm 20j$. Figure 7 shows the root locus for the two compensated transfer functions, where $\omega_n = 37.1$ and 3.71:

$$\frac{T_L}{\omega_m} = \frac{1780^2 \cdot 138 / 156(s + 40 + 800)}{s(s^2 + 3130s + 1780^2)(s^2 + \omega_n^2)}$$

The root locus shown in Figure 7 is used to calculate a suitable gain for this compensator. With a gain of 500, the dominant poles of the system have frequency of 840 rad/s and a damping ratio of 0.77. The assumption of dominance of the poles is supported by calculating the residues for the closed loop transfer function. Table 2 shows the residues; two poles cancel the compensator zeroes, leaving the fast acting poles to dominate the transient response. The load on the SEA has little impact on the response. This is further illustrated by the step response shown in Figure 8. The frequency response shown in Figure 9 is flat until it approaches the closed loop poles at 840 rad/s.

Table 2: Residues for large and small load showing dominance of fast acting poles.

	Load (kgm ²)	p ₁	p ₂	p ₃	p ₄	p ₅
Residue	J=0.1	-3.1±1.2j		-443±951j		893
Pole	J=0.1		-23±19j		-650±535j	-1785
Residue	J=10	-1.1±1.1j		-445±944j		892
Pole	J=10		-21±21j		-651±536j	-1785

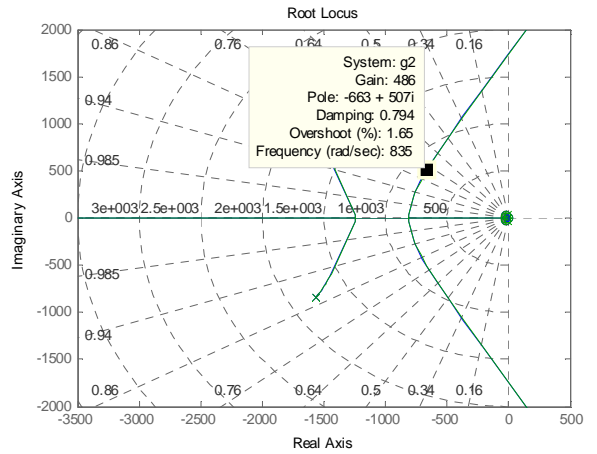


Figure 7: Root locus for both large and small loads overlaid. There is very little movement in the system for a change in load.

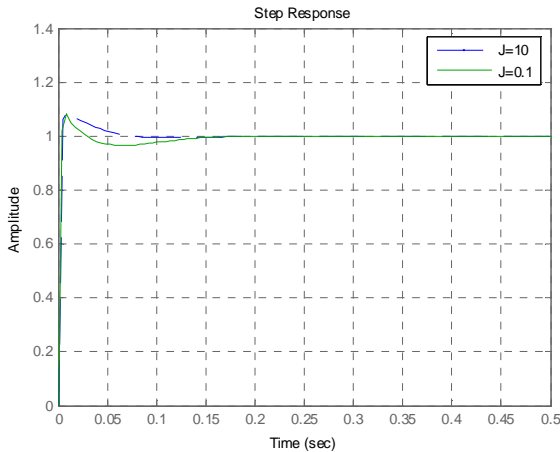


Figure 8: Step response to a torque command for large and small loads.

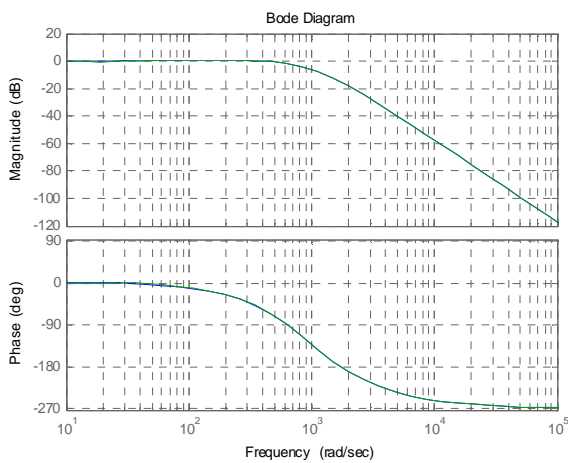


Figure 9: Bode plot for large and small loads.

6 Non-Linear and Discrete Elements

It is apparent from previous work that the non-linear and discrete components inherent in any practical implementation of an SEA can have undesirable effects on the performance. In this section we evaluate the performance of the SEA with the following non-linear and discrete time components added to the system:

- A digital controller sampling at 3.6 kHz, which is the fastest sampling rate limit of the slowest element (the magnetic angle sensor).
- Quantisation of the magnetic angle sensor.
- Quantisation and discrete derivative effects of the optical encoder.
- Voltage saturation in the motor amplifier.
- Stiction in the motor drive train.

Also the effects of loading from output on the motor velocity control loop were considered as part of this study; motor loading was assumed negligible in the linear analysis. These elements were tested by evaluating an extensive model in Simulink. Implementation of the model required some consideration. Before discussing the results, those implementation issues are discussed here.

6.1 Digital Controller Design

Given that the control loop runs at 3.6 kHz, well above the frequencies of the system under control, the digital

controller was designed by a simple linear to discrete substitution. The gains calculated from the linear design process were substituted directly into discrete time equivalents. The motor velocity controller was implemented by:

$$K_p + \frac{K_i}{s} \Rightarrow K_p + \frac{K_i T_s z}{z-1}$$

$$0.27 + \frac{54}{s} \Rightarrow 0.27 + \frac{(54/3600)z}{z-1}$$

Similarly the SEA controller was implemented by:

$$500 \left(1 + \frac{40}{s} + \frac{800}{s^2} \right) \Rightarrow 500 \left(1 + \frac{(40/3600)z}{z-1} + \frac{(800/3600^2)z^2}{(z-1)^2} \right)$$

This controller can be implemented in cascade form as shown in Figure 10. The cascade form simplifies coding of the controller.

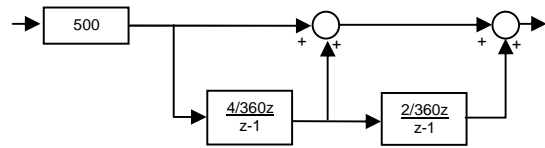


Figure 10: Cascade implementation of compensator with complex conjugate zeros.

6.2 Non-linear Elements

The quantisation of the magnetic sensor was set to 0.02° / bit, which is conservative based on sensor data which quotes 0.01° / bit. The encoder angle was quantised at 2000 counts per revolution, based on reading every edge created by the quadrature decode process. A discrete derivative was implemented to extract to velocity information at the system sampling rate. The motor voltage saturation was set to ± 50 V. The gear box was given a Coulomb friction value of 1 mNm (at the motor) and a viscous friction of 0.72 (gain). The Coulomb friction value is a generous estimate (the real value is likely much lower), with the viscous friction based on the manufacturer's rated gear-box efficiency.

6.3 Results

Data was gathered from Simulink to compare the step response and frequency response of the non-linear and discrete system to the linear system designed in the previous section. The first key result is the step response of the system, as shown in Figure 11.

The similarity between Figures 8 and 11 is high, justifying the assumptions made in the design. Most of the non-linear and discrete effects have been reduced to have negligible impact on the step response. There is clearly some impact from quantisation noise on the steady state response, and the overshoot is slightly larger than predicted. Nevertheless this result compares well to others published in the literature.

Frequency response data was gathered by exciting the system with a 2 Nm pk-pk sine wave representing the desired torque. The magnitude and phase were recorded for the output torque over a range of frequencies and plotted in Figure 12. The experimental Bode plot reveals that the dominant pole positions have moved from the linear analysis. The poles appear at a slightly lower frequency (500 rad/s), and appear to have a lower damping ratio by the steepness of the phase plot.

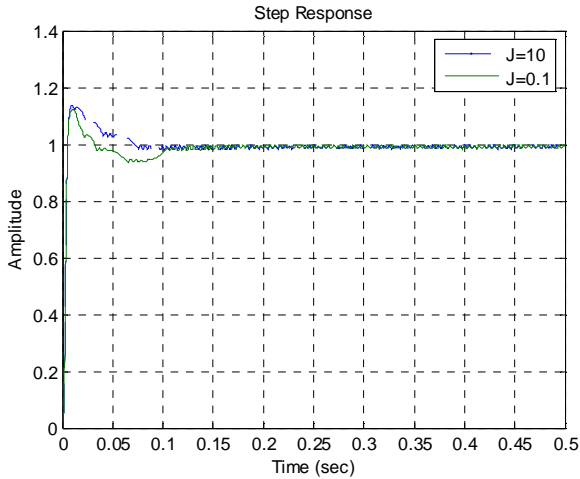


Figure 11: Step response from simulation including all non-linear and discrete elements.

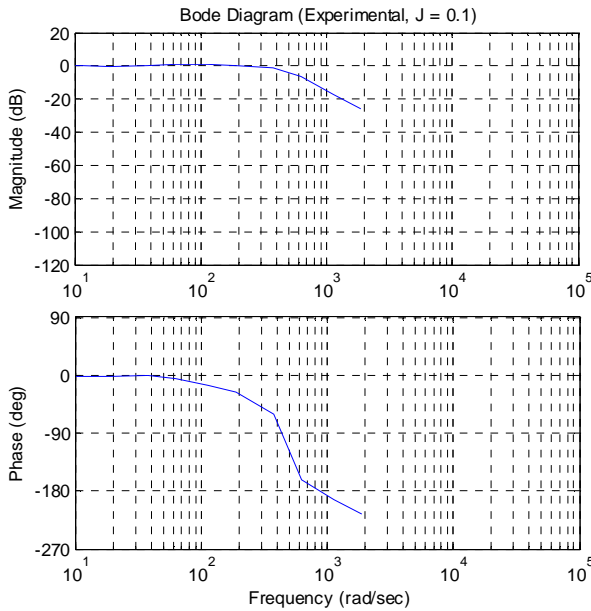


Figure 12: Bode plot from experimental data.

7 Conclusions

Series Elastic Actuators show great promise in increasing the inherent safety of human robot interaction. However, past implementations of SEAs have run into difficulties when the electric motor is treated as a torque source using current control. This paper has shown that by treating the motor as a velocity source by using tight encoder feedback, many of the problems inherent in current control of motors disappear and the performance of the SEA is greatly improved. The paper presents a new control method using cascaded PI compensators that is simple to implement and highly effective. Results from

high quality simulation show that non-linear effects have little impact on the system when the velocity sourced SEA is controlled in this fashion.

7.1 Future Work

The SEA described in Section 4 is being constructed as this paper is written. We will have results from the real hardware before the conference. There also needs to be some continuing work in simulation to assess the inherent safety in the proposed design. While the output impedance clearly reduces to that of the spring at high frequencies, it remains to be seen whether this is enough to prevent injury for a usefully sized robot actuator.

Acknowledgements

The author gratefully acknowledges the contribution of Patrick Collis in the mechanical design and drafting of the series elastic element, and Jebran Hussain in the initial modelling of the motor and SEA.

References

- [Brooks *et al*, 1998] Brooks, R., C. Breazeal, M. Marjanovic, B. Scassellati, and M. Williamson, *The Cog Project: Building a Humanoid Robot*, in *Computation for Metaphors, Analogy and Agents*. 1998, Springer-Verlag.
- [Paluska, 2000] Paluska, D.J., *Design of a Humanoid Biped for Walking Research*, Master of Science Thesis, Department of Mechanical Engineering, Massachusetts Institute of Technology, 2000.
- [Pratt and Williamson, 1995] Pratt, G.A and Williamson, M.M *Series Elastic Actuators*, Proc. of International Conference on Robotic Systems 1995 (IROS 1995), p. 399 - 406
- [Pratt *et al*, 2004] Pratt, G.A., P. Willisson, C. Bolton, and A. Hofman. *Late Motor Processing in Low-Impedance Robots: Impedance Control of Series Elastic Actuators*. in Proc of American Control Conference. 2004. Boston, MA.
- [Robinson *et al*, 1999] Robinson, D.W., J.E. Pratt, D.J. Paluska, and G.A. Pratt. *Series Elastic Actuator Development for a Biomimetic Walking Robot*. in IEEE/ASME Int'l Conf. On Adv. Intelligent Mechatronics. 1999.
- [Robinson, 2000] Robinson, D.W. *Design and Analysis of Series Elasticity in Closed-loop Actuator Force Control*, PhD Thesis, Department of Mechanical Engineering, Massachusetts Institute of Technology, 2000.
- [Williamson, 1995] Williamson, M.M., *Series Elastic Actuators*, Master of Science Thesis, Department of Electrical Engineering and Computer Science, Massachusetts Institute of Technology, 1995.
- [Zinn *et al*, 2004] Zinn, M., O. Khatib, B. Roth, and J.K. Salisbury, *Playing It Safe*. IEEE Robotics and Automation Magazine, 2004. 11(2): p. 12-21.